

# Sarcopenia is not due to lack of regenerative drive in senescent skeletal muscle

Erik Edström and Brun Ulfhake

Department of Neuroscience, Karolinska Institutet, S171 77 Stockholm, Sweden

## Summary

**Sarcopenia, loss of skeletal muscle mass, is a hallmark of aging commonly attributed to a decreased capacity to maintain muscle tissue in senescence, yet the mechanism behind the muscle wasting remains unresolved. To address these issues we have explored a rodent model of sarcopenia and age-related sensorimotor impairment, allowing us to discriminate between successfully and unsuccessfully aged cohort members. Immunohistochemistry and staining of cell nuclei revealed that senescent muscle has an increased density of cell nuclei, occurrence of aberrant fibers and fibers expressing embryonic myosin. Using real-time PCR we extend the findings of increased myogenic regulatory factor mRNA to show that very high levels are found in unsuccessfully aged cohort members. This pattern is also reflected in the number of embryonic myosin-positive fibers, which increase with the degree of sarcopenia. In addition, we confirm that there is no local down-regulation of IGF-I and IGF-IR mRNA in aged muscle tissue; on the contrary, the most sarcopenic individuals showed significantly higher local expression of IGF-I mRNA. Combined, our results show that the initial drive to regenerate myofibers is most marked in cases with the most advanced loss of muscle mass, a pattern that may have its origin in differences in the rate of tissue deterioration and/or that regenerating myofibers in these cases fail to mature into functional fibers. Importantly, the genetic background is a determinant of the pace of progression of sarcopenia. Key words: aging; fiber type; IGF; MHC; MRF; satellite cell.**

## Introduction

During aging, humans lose about one-third of the skeletal muscle mass, a process referred to as sarcopenia (Rosenberg, 1997) or 'senile muscle atrophy' (Gutman & Hanzlikova, 1972). A key issue in sarcopenia is whether aged skeletal muscle is undergoing a programmed atrophy or whether it is wasting away due to circumstances with which it cannot cope. Mature

skeletal muscle fibers are post-mitotic and depend on the recruitment of muscle precursor cells (MPCs) via growth factors such as IGF-I for regeneration and growth (Robertson *et al.*, 1993; Allen *et al.*, 1996; Tureckova *et al.*, 2001; Vandromme *et al.*, 2001). A number of studies have reported increased levels of myogenic regulatory factors (MRFs; Musaro *et al.*, 1995; Dedkov *et al.*, 2003), which are essential for the normal formation and maturation of skeletal muscle, suggesting that the senescent tissue is in a state of regeneration. To address these questions we describe here the establishment of an animal model for the study of sarcopenia that allows us to distinguish between successful and unsuccessful aging phenotypes, and relate them to behavioral motor impairment as well as to the degree of sarcopenia and morphological alterations.

Applying real-time PCR and immunohistochemistry to our model we have analysed sarcopenic rodent hind limb muscle (*triceps surae*, comprising *m. soleus* and *m. gastrocnemius*) to determine to what extent regeneration characterizes successful and unsuccessful patterns of skeletal muscle aging.

## Results

### Sarcopenia index

The sarcopenia index (SI) is used as a measure of how well adapted the soleus muscle is in performing its weight-bearing task, and as such the SI reflects the success or failure to maintain muscle mass in relation to body weight in aged sarcopenic animals (Fig. 1: ANOVA  $P < 0.001$ ; for results of Bonferroni's *post-hoc* test see Fig. 1). As shown in Fig. 1 there is an increase in SI from adolescence to adulthood and a decline of SI in senescence. The 4-month-old controls were not significantly different from the 12-month-old rats (Bonferroni's *post-hoc* test: 4 month vs. 12 month,  $P = 1$ ), and both the 4-month-old and the 12-month-old rats were different from the aged animals (30 months old) in the high (AgH) and low (AgL) symptom groups (Bonferroni: 12 month vs. 30 month AgL,  $P < 0.001$ ; 12 month vs. 30 month AgH,  $P < 0.001$ ). Moreover, there was a significant difference in the SI of the low and the high symptom groups of aged rats (Fig. 1).

In addition, the 12-month group was different from the 2-month group (Bonferroni's *post-hoc* test: 2 month vs. 12 month,  $P < 0.01$ ), a difference that was only a trend between the two younger age groups (2 month vs. 4 month,  $P = 0.054$ ). The youngest age group displayed relatively low SI values, but was nonetheless more similar to the 4- and 12-month-old than to the aged animals, and thus significantly different from these groups (Bonferroni: 2 month vs. 30 month AgL,  $P < 0.001$ ; 2 month vs. 30 month AgH,  $P < 0.001$ ).

### Correspondence

Dr Erik Edström, MD, Experimental Neurogerontology, Department of Neuroscience, Retzius väg 8 A3:4, 171 77 Stockholm, Sweden. Tel.: +46 8 5248 78 99; fax: +46 8 33 39 68; e-mail: erik.edstrom@neuro.ki.se

Accepted for publication 17 January 2005

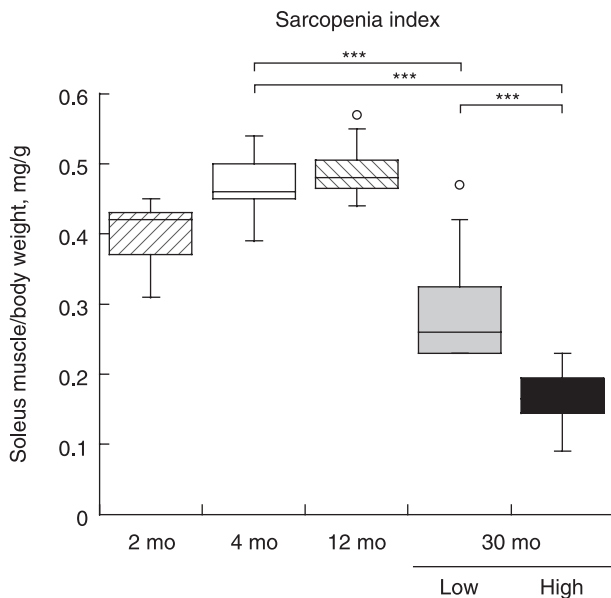


**Fig. 1** Sarcopenia index (soleus muscle weight/body weight; mg/g) plotted for rats of different ages. Brackets and corresponding legends indicate results of statistical evaluation (*post-hoc*-test) of data. Note that only results of statistical comparisons of 4-month-old ( $n = 10$ ) and 30-month-old animals with low (AgL;  $n = 12$ ) and high (AgH;  $n = 8$ ) symptoms of motor impairment are shown. For the other comparisons, see text in the results section.

### Behavioral signs of impaired muscle function in senescent rats

All behavioral data were statistically analysed in two steps. An overall test on the three groups, 4-month-old adult (Ad) and 30-month-old low symptom (AgL) and high symptom (AgH), was performed using Kruskal–Wallis analysis of variance (KWA). When this test showed significant differences, multiple comparisons (MC) were used to verify which groups differed (see Experimental procedures). To simplify the presentation of the behavior analysis results, significant differences are illustrated in the figures and not repeated in the text, while comparisons not included in the figures are found in the text. Non-significant differences are not presented separately with the exception of overall KWA results. Aged animals showed a general decline in explorative behavior evident in the open field test (KWA,  $P < 0.001$ ; Fig. 2A), a result that seems to be independent of level of anxiety (KWA,  $P = 0.21$ ; Fig. 2B). A similar age-related decline was seen in the number of rearings performed (KWA,  $P < 0.001$ ; MC: Ad vs. AgL,  $P < 0.001$ ; Ad vs. AgH,  $P < 0.001$ ), while a corresponding age-related increase was seen in the occurrence of immobility periods during exploration of the open field (KWA,  $P < 0.001$ ; MC: Ad vs. AgL,  $P < 0.001$ ; Ad vs. AgH,  $P < 0.001$ ). Overt signs of hind limb incapacitation were seen in the mesh walk of aged rats in the high symptom group, but not in aged animals with a successful pattern of aging (KWA,  $P < 0.001$ ; Fig. 2C). Likewise, high symptom animals scored poorly in the beam balance test whereas adults scored well and

aged low symptom animals scored in between these two groups (KWA,  $P < 0.001$ ; Fig. 2D). When time on the beam was analysed, however, the aged groups were both significantly different only when compared with adults (KWA,  $P < 0.001$ ; MC: Ad vs. AgL,  $P < 0.001$ ; Ad vs. AgH,  $P < 0.001$ ). The gait analysis showed a decrease in stride length, manifest only in high symptom rats (KWA,  $P < 0.001$ ; Fig. 2E). Increased placement difference and gait width appear to be early signs of impairment and were evident also among successfully aged rats (placement: KW,  $P < 0.001$ ; MC: Ad vs. AgL,  $P < 0.001$ ; Ad vs. AgH,  $P < 0.001$ ; width: KW,  $P < 0.001$ ; MC Ad vs. AgL,  $P < 0.001$ ; Ad vs. AgH,  $P < 0.01$ ). Whole body agility and control, tested in the righting response, confirmed the pattern of behavioral decline among the aged animals (KWA,  $P < 0.001$ ; Fig. 2F). Combined, these tests show that 30-month-old rats are not a homogeneous group, and that the performance of successfully aged rats did not deviate significantly from that of adult controls in several of the tests.

### Aged skeletal muscle and signs of regeneration

Aged soleus muscle displays an array of histological alterations. These changes seem to relate more to the degree of motor impairment of the animal than to chronological age. Thus, changes described as age-related are most prominent in unsuccessfully aged animals and may be very discrete or even lacking in successfully aged animals. Aged soleus muscle shows an accumulation of nuclei (Fig. 3A,D), a wide distribution of fiber sizes (Fig. 3E–G, see also Fig. 4B) and a conspicuous pattern of staining for fast and slow myosin isoforms (Fig. 3E,F). An antibody to laminin used to stain the muscle basement membrane revealed that a large fraction of the supernumerary nuclei were located to the myofiber compartment (Fig. 4). These nuclei were often more rounded and frequently located to the central region of the muscle fiber (arrows in Fig. 3D). In order to examine if the increased number of mononuclear cells with a location outside muscle fibers also derived from fibroblasts, resident or invading inflammatory cells, selective markers for these cell lines were employed. While labeling with an antibody directed against proline hydroxylase (fibroblasts) failed, antibodies directed against ED1 and ED2 showed a modest increase in ED2-immunopositive cell profiles in aged muscle of high symptom animals (Fig. 5), indicating an increase in cells with poor phagocytic capacity.

In aged muscle, dense clusters of nuclei were found superimposed on groups of small fibers (Fig. 4B,D,F). These groups of small fibers (Fig. 3E–G) and morphologically aberrant fibers (Fig. 6) are also apparent when staining for fiber types in aged muscle. Fast and slow fiber types are easily distinguished in young muscle and there are no fibers positive for both isoforms (Fig. 3B,C). In aged muscle, however, small-diameter fibers are frequently seen forming groups immunopositive for MHCf and MHCe set against a background of MHCs-positive fibers (Fig. 3E–G). Furthermore, and in agreement with previously published data, there seems to be a general shift towards the slow MHC isoform and a dedifferentiation evident in a large number of

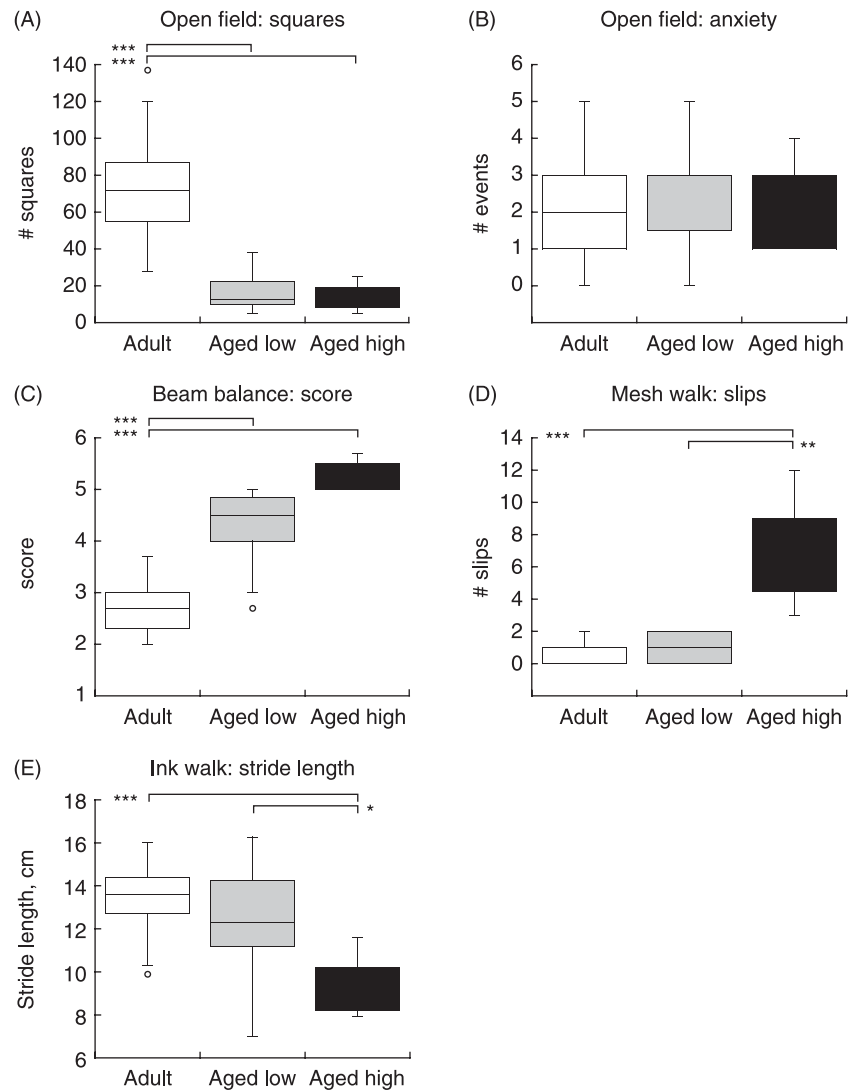


**Fig. 2** Behavioral testing of 4-month-old adult ( $n = 30$ ) and 30-month-old (aged) animals divided into low (AgL;  $n = 16$ ) and high (AgH;  $n = 9$ ) symptom groups based on global assessment of muscle function impairment. (A) Number of squares ( $14 \times 14$  cm) entered during 3 min of explorative activity in the open field test. A general reduction in explorative activity is seen in the aged animals. (B) Estimated anxiety (instances of urination and defecation) level during the open field test. Analysis reveals no difference between the different groups. (C) Impairments in coordination, postural control and balance, as probed in the beam balance test. Scores up to three represent balancing on the beam for the full trial period of 60 s, while scores above three represent failure to stay on the beam. A score of six represents little or no attempt at balancing. Analysis shows an increase in the aged animals and are more pronounced in the high symptom (AgH) group. (D) Signs of poor hind limb coordination are assessed as number of errors in hind paw placement (slips) while traversing a wire mesh screen. This parameter increases in the aged high symptom (AgH) group. (E) A decrease in hind limb stride length occurs with aging and becomes pronounced in the high symptom (AgH) group.

fibers in aged muscle (Fig. 3E–G). Dedifferentiated fibers display less intense immunolabeling and/or are immunopositive for more than one MHC isoform, including MHCE (Fig. 3E–G, see also Fig. 6). In skeletal muscle of adult rats, few if any fibers are positive for the embryonic MHC isoform, whereas a considerable number of positive fibers are found in aged muscle (Figs 3G and 7A–C). The number of MHCE-positive fibers was higher in aged than in adult rats (ANOVA,  $P < 0.001$ ; for results of Bonferroni tests, see Fig. 7D). Moreover, the numbers increased significantly in AgH compared with AgL samples (for results of Bonferroni tests, see Fig. 7D). In aged animals the MHCE immunolabeling was graded (Fig. 7B,C) and fibers with relatively lower levels were often more similar in size to fibers expressing mature MHC isoforms.

### Increased expression of MRFs in aged skeletal muscle

Strongly increased expression levels of MyoD and myogenin mRNA were found in aged gastrocnemius muscle (ANOVA: MyoD,

$P < 0.001$ ; myogenin,  $P < 0.001$ ; Fig. 8). However, the aged AgL and AgH animal groups were not statistically different from each other (Fig. 8). MRF4 and Myf5 levels were increased only in the AgH animals (ANOVA: MRF4,  $P < 0.05$ ; Myf5,  $P < 0.05$ ; Fig. 8). Overall, a strong trend towards increased expression of the MRFs is evident in senescent skeletal muscle.

### Expression of IGF signaling components

Pre-pro IGF-I mRNA was increased in the gastrocnemius skeletal muscle of AgH aged animals but not in the AgL animals (ANOVA: AgH vs. Ad,  $P < 0.001$ ; Fig. 9). IGF-I signals via the IGF-I receptor (IGF-IR), but only the low symptom animals showed a small up-regulation (ANOVA: AgL vs. Ad,  $P < 0.01$ ; Fig. 9). IGF binding protein 5 (IGFBP5) mRNA levels in gastrocnemius muscle were increased in the low symptom aged animals and showed a tendency for up-regulation in high symptom aged animals (ANOVA:  $P < 0.001$ ; Bonferroni: Ad vs. AgH,  $P = 0.07$ ; Fig. 9).

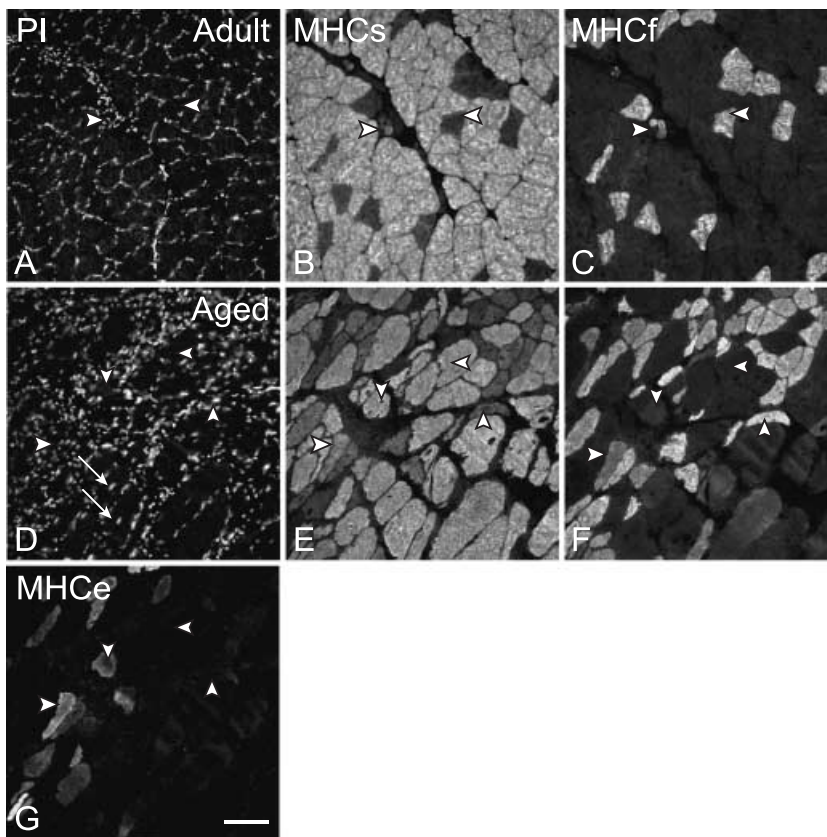


**Fig. 3** Nuclear staining using propidium iodide (PI) and immunohistochemical staining for fast, slow and embryonic myosin heavy chain (MHC) isoforms in soleus muscle cross-sections of 4-month-old adult (Ad; A–C) and 30-month-old aged (Ag; D–G) animals. In adult animals (A) an orderly pattern of staining for all markers is seen: myofibers have a modest variation in diameters and nuclei locate to the periphery of fibers, which stain strongly for either slow or fast MHC (B,C). Note that no fibers co-expressing MHCs and MHCf are seen in the adult. None of the fibers shown in adult was MHCe positive (not shown). Arrowhead pointing right in A–C indicates MHCf-positive intrafusal fibers, while the left-pointing arrowhead indicates typical MHCs-negative and MHCf-positive myofibers. In aged animals the muscle organization has changed and suggests ongoing regeneration: fiber diameters vary, increased numbers of nuclei with locations varying from the periphery to the center of myofibers (arrows in D) and MHCe-positive fibers are seen (G). Fiber isoform clustering is seen as well as fibers co-expressing MHC isoforms (E–G). Arrowheads indicate: (pointing left) large exclusively MHCs-positive fiber, (pointing up) slender MHCf-positive fiber, (pointing down) MHCs- and MHCe-positive fiber, (pointing right) thin MHCs-, MHCf- and MHCe-positive fiber. Scale bar represents 100  $\mu$ m for all images.

## Discussion

Our results show that the rodent model of sarcopenia used here shares strong similarity with available data on the human counterpart (Dutta & Hadley, 1995; Jette & Jette, 1997; Rosenberg, 1997; Roubenoff & Castaneda, 2001) and should therefore be a useful model for further experimental research on aging-related loss of skeletal muscle tissue. Furthermore, we show here at the tissue as well as the cellular level that there is no lack of regenerative drive underlying sarcopenia. Still, muscle wasting progresses and below we discuss whether this pattern results from the pace of tissue damage exceeding that of repair, and also whether the late phase of myofiber regeneration fails in senescence. Finally, the results clearly indicate that genetic background is one of the determinants of the sarcopenic process.

### Characterization of rat sarcopenia

Combined with other classical markers of human aging, sarcopenia results in clinically relevant behavioral impairments that put the elderly at risk of fall-related injuries (Evans, 1995; Jette & Jette, 1997). Our data clearly show that aging rats also become behaviorally impaired in senescence and that at least the Sprague–Dawley strain suffers from sarcopenia. In fact, the results indicate a strong association between degree of sarcopenia and the extent of the motor behavior disturbances as indicated by the differences between high and low symptom groups of aged

rats. The SI used here reflects the failure to maintain muscle mass in relation to body weight in the aged animals. Our data also show that, although living conditions remain unchanged, the SI is subject to changes during adolescent development up to an age of 3–4 months after which it appears to be stable over at least the first year of life. This observation stresses the importance of a multiple time-point design in studies of aging.

The loss of muscle mass in sarcopenia is the net effect of fiber loss and fiber atrophy (Gutman & Hanzlikova, 1972; Caccia *et al.*, 1979; Porter *et al.*, 1995), which preferentially affects fast type fibers (Lexell, 1995). At the cellular level, our results are consistent with earlier studies, and the sarcopenic muscle displays a dominance of slow type fibers and a loss of isoform fidelity as well as fiber atrophy and fiber type grouping (Tomonaga, 1977; Larsson, 1978; Klitgaard *et al.*, 1990; Lexell, 1995; Andersen *et al.*, 1999; Williamson *et al.*, 2000). Most commonly, these aging-related changes, which are typical for skeletal muscles, have been attributed either to an impaired innervation (neurogenic origin), an inadequate regeneration of muscle fibers (intrinsic origin) or endocrine failure (systemic origin) (for recent reviews of sarcopenia etiologies, see, for example, Greenlund & Nair, 2003; Marcell, 2003).

### Sarcopenia and myofiber regeneration

Mature skeletal muscle fibers contain post-mitotic and terminally differentiated nuclei with a relatively fixed, fiber-type-specific,

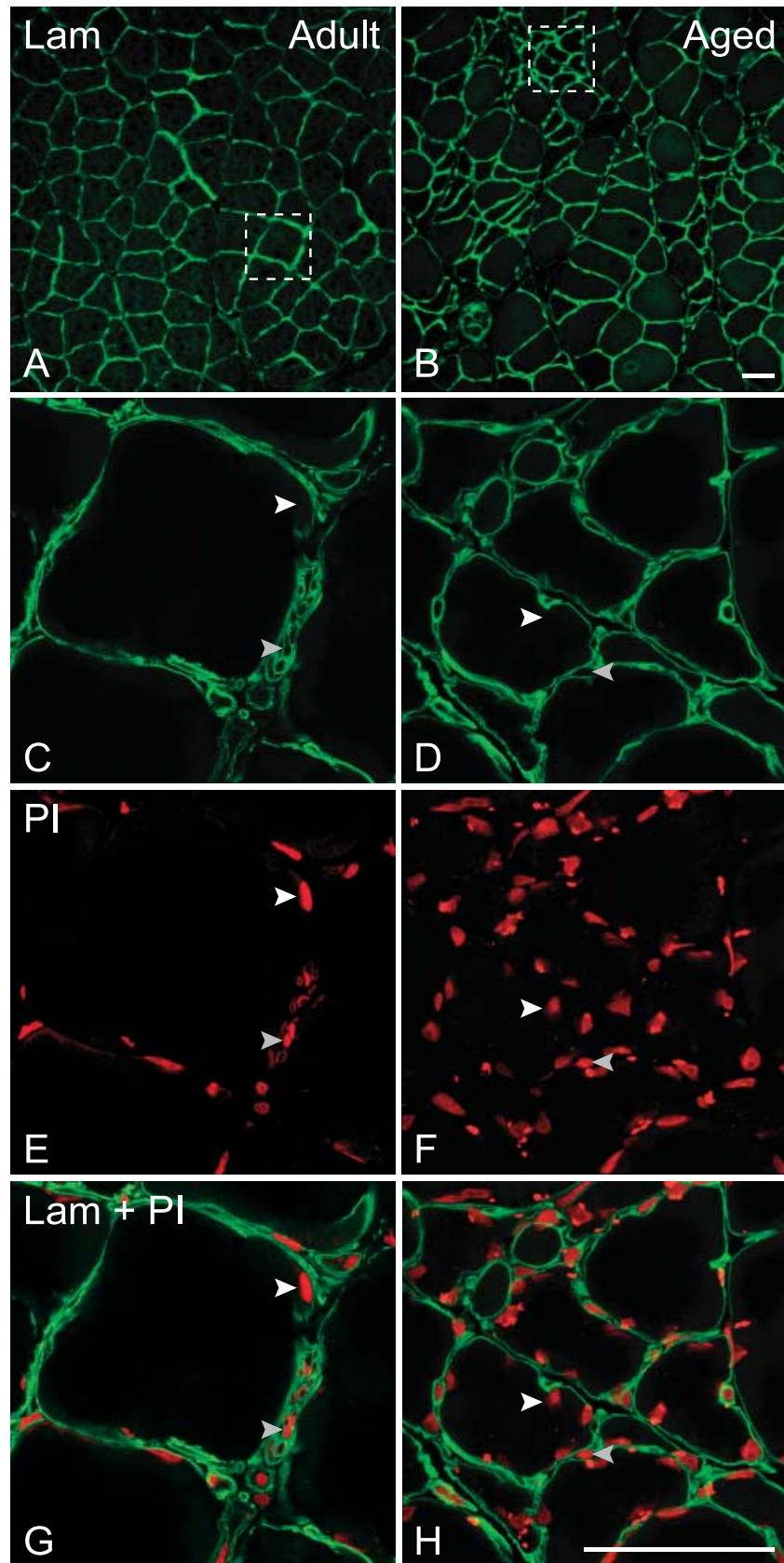


**Fig. 4** Double staining in soleus muscle cross-sections of 4-month-old adult (Adult; A, C, E, G) and 30-month-old aged (Aged; B, D, F, H) animals using propidium iodide (PI) and anti-laminin (Lam) immunohistochemistry (IHC), to identify cell nuclei and the myofiber basement membranes, respectively. Overview images of laminin IHC show the differences in skeletal muscle organization between adult and aged animals (A, B), and indicate areas (with dashed border) shown at higher magnification in the subsequent images (C–H). Deviating from the organized pattern of adult muscle, a wide distribution of fiber diameters is seen in the aged animals and includes groups of fibers with very small diameters (B, D). Laminin IHC is shown in a group of small fibers in aged muscle (D) and a similarly sized area in adult muscle (C) alongside their corresponding double staining with PI (adult: E; aged: F). In order to allow discrimination of the location of nuclei relative to the perimeters (basement membranes) of the myofibers, laminin and PI images are superimposed (adult: G; aged H). Note the increased density of nuclei in aged (F) compared with adult muscle (E), and how the supernumerary nuclei locate to the myofiber compartment (G). The white arrowheads indicate nuclei located to the myofiber compartment, while the gray arrowheads indicate nuclei located to the outside of the myofiber compartment (C–H). The nuclei indicated by the gray rightward-pointing arrowhead probably represent cells of a capillary wall extending across the side of the myofiber (C, E, G). Scale bar in B represents 50  $\mu\text{m}$  for A and B, while scale bar in H represents 50  $\mu\text{m}$  for all other images (C–H).

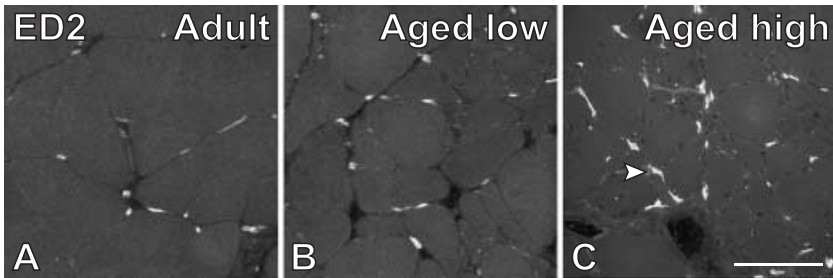


**Fig. 5** Immunohistochemical ED2 staining of soleus muscle cross-sections. ED2 antigen is expressed on a subset of inflammatory cells with poor phagocytic capacity. ED2-positive cell profiles are localized to the interstitial space in 4-month-old adult (A) and low (AgL; B) as well as high (AgH; C) symptom aged animals (30-month-old). Increased numbers of ED2-positive cells are seen in the AgH (C) group as compared with the AgL (B) and adult (A) groups. Arrowhead indicates ED2-positive inflammatory cell extending processes into adjacent connective tissue regions (C). Scale bar represents 50  $\mu$ m for A–C.

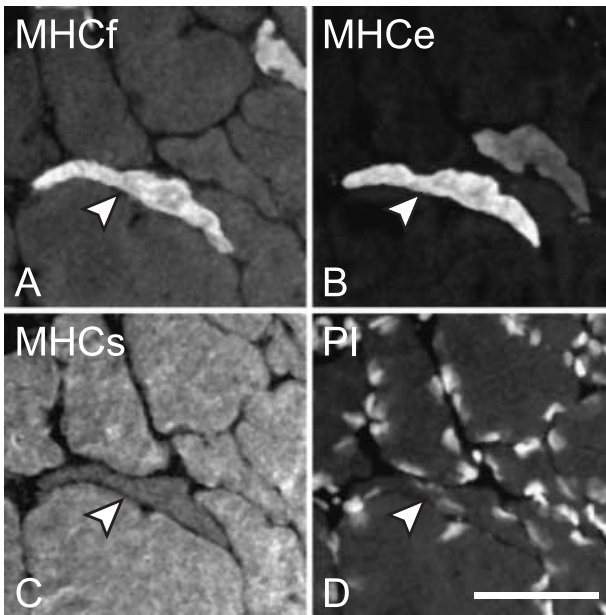


**Fig. 6** Immunohistochemical staining for fast (f), embryonic (e) and slow (s) myosin heavy chain (MHC) isoforms in soleus muscle cross-sections from aged animals (30-month-old). Arrow indicates slender MHCf- (A) and MHCe- (B) positive fiber extended around the perimeter of an adjacent fiber. The slender fiber is MHCs negative (C). Propidium iodide (PI) staining shows nuclei located within the fiber profiles (D). Scale bar represents 50  $\mu$ m for all images.

relation between myofiber size and myonuclear number (Allen *et al.*, 1995; Chambers & McDermott, 1996). Myonuclear domains are maintained even during rapid atrophy (Hikida *et al.*, 1997) and increased density of nuclei is therefore interpreted as the addition of new nuclei through MPC proliferation, rather than selective atrophy with sparing of myonuclei. Conversely, mature hypertrophic skeletal muscle must recruit additional nuclei in order to maintain the myonuclear domains. Satellite cells are believed to be the primary source of additional myonuclei in mature skeletal muscle and are recruited after muscle overload, denervation or experimental damage to the muscle (Robertson *et al.*, 1993; Allen *et al.*, 1996). In these situations, changes in the local environment, including the production of growth factors, activate quiescent satellite cells to a proliferative state. Several growth factors, such as IGF-I, hepatocyte growth factor, fibroblast growth factor, interleukin-6 and leukemia inhibitory factor, have

been shown to stimulate satellite cell proliferation (reviewed in Hawke & Garry, 2001). A common notion has been that muscle function impairment and muscle wasting during aging are caused by incapacitation of the GH–IGF-I axis. However, available evidence indicates that skeletal muscles are dependent on auto- and paracrine IGF-I rather than liver-derived IGF-I. Neither hypophysectomy (Adams & Haddad, 1996) nor targeted inactivation of liver IGF-I (Sjogren *et al.*, 1999) apparently results in lack of skeletal muscle growth. Following the same line of evidence, clinical trials with systemic GH and/or IGF-I treatment have, by and large, failed to increase muscle mass in the elderly (Lieberman & Hoffman, 1997; Friedlander *et al.*, 2001), while transgenic (Musaro *et al.*, 2001) or vector-mediated (Barton-Davis *et al.*, 1998) over-expression of IGF in muscle appears to attenuate the loss of muscle mass in senescence. These data stress the significance of local IGF over systemic IGF, a notion compatible with the longevity phenotype of mice with mutated growth hormone receptor or IGF-I receptor (Coschigano *et al.*, 2000; Holzenberger, 2004). In line with previous data (Hamilton *et al.*, 1995; Severgnini *et al.*, 1999), we find no local down-regulations of pre-pro IGF-I, IGF-IR or IGFbp5 (for IGF binding proteins see Chan & Spencer, 1997). In contrast, among the high symptom aged rats a significant increase in pre-pro IGF-I mRNA level was evident; aged skeletal muscles also showed an up-regulation of IGFbp5. IGFbp5 is involved in the specification of the muscle lineage during development (McQueeney & Dealy, 2001), and is up-regulated in skeletal muscle in response to IGFs (Rotwein *et al.*, 1995). Our data indicate that IGFbp5 may also have a role in muscle regeneration during aging (Foulstone *et al.*, 2001).

Intact local IGF signaling is consistent with the increased number of cell nuclei seen here in the aged sarcopenic muscle. The modest increase in ED2-positive cells and unchanged content of ED1-positive cells in aged muscle argue against the supernumerary nuclei representing an inflammatory infiltrate. Instead we suggest that a substantial part of these supernumerary nuclei represent MPCs, because they locate to the myofiber compartment. Co-localization of MHCe and supernumerary nuclei as well as the location of nuclei to the central portion of muscle fibers strengthens the case for a role for these cells in muscle regeneration.

Activated satellite cells and their offspring MPCs seem to replicate parts of the embryonic program of muscle formation, including the expression of MRFs (Hawke & Garry, 2001) during

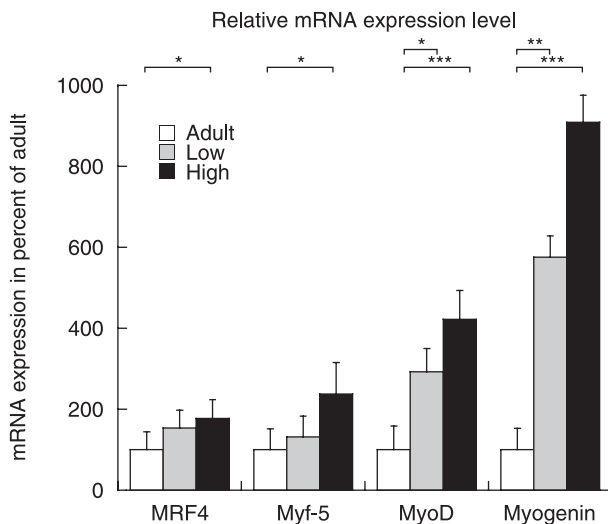
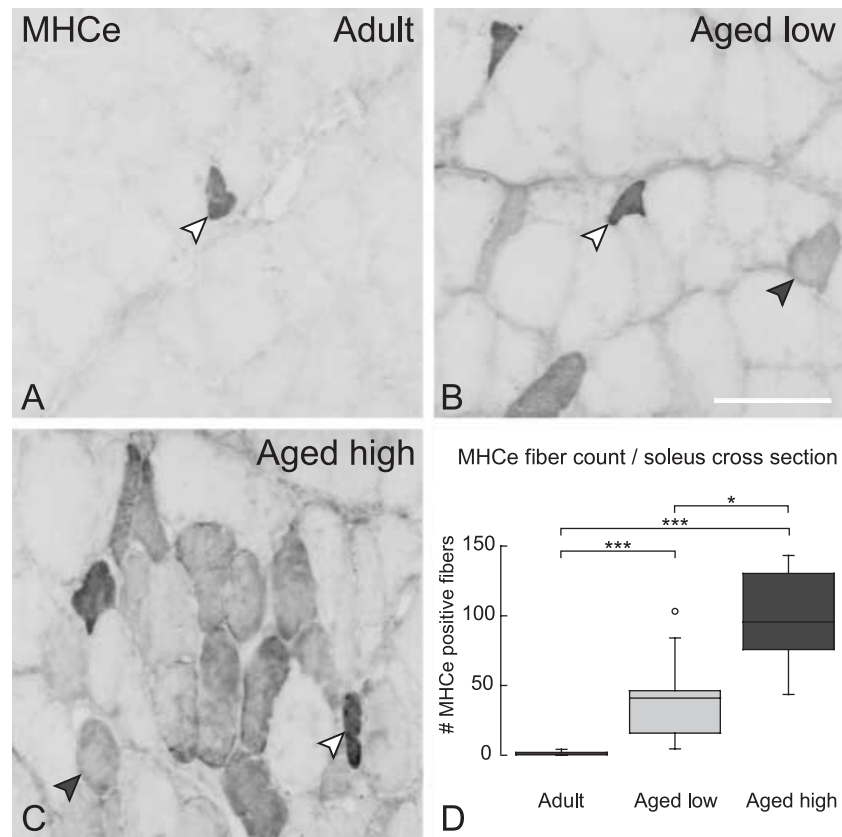


**Fig. 8** Results of real-time PCR analysis of MRF4, Myf-5, MyoD, myogenin and  $\beta$ -actin in gastrocnemius muscle of adult (4 months old,  $n = 10$ ), AgL ( $n = 8$ ) and AgH ( $n = 7$ ) groups. Relative mRNA expression levels, normalized to  $\beta$ -actin, are expressed in percent of adult (standardized to 100%). Error bars indicate SD. Brackets and corresponding legends indicate results of statistical evaluation (Bonferroni's *post-hoc* test) of data. Non-significant differences are not illustrated.

tissue regeneration. The MRF proteins include myogenin, Myf-5, MyoD and MRF4. During development the order of expression of the MRF genes varies depending on muscle origin and species (Ludolph & Konieczny, 1995; Yun & Wold, 1996), and a similar

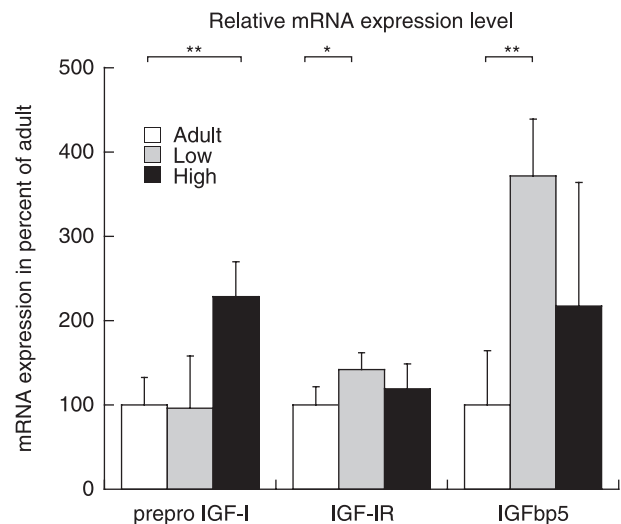


**Fig. 9** Results of real-time PCR analysis of pre-pro IGF-I, IGF-IR, IGFbp5 and  $\beta$ -actin in gastrocnemius muscle from adult (4 months old,  $n = 10$ ), AgL ( $n = 8$ ) and AgH ( $n = 7$ ) groups. Relative mRNA expression levels, normalized to  $\beta$ -actin, are expressed in percent of adult (standardized to 100%). Error bars indicate SD. Brackets and corresponding legends indicate results of statistical evaluation (Bonferroni's *post-hoc* test) of data.

hierarchy is seen in regeneration (Launay *et al.*, 2001). MyoD and Myf-5 are necessary in specification of the myogenic lineage (Rudnicki *et al.*, 1993; Tajbakhsh *et al.*, 1996; Kablar *et al.*, 1997). Myogenin and either MyoD or MRF4, by contrast, are required

for differentiation (Hasty *et al.*, 1993; Smith *et al.*, 1993; Rawls *et al.*, 2000). It has been suggested that increased levels of MRFs maintain the differentiated phenotype of skeletal muscle during senescence (Musaro *et al.*, 1995). Based on our results showing an up-regulation of MRFs in parallel with increased tissue wasting in senescent muscle, we suggest instead that the increased MRF levels reflect a regenerative drive that is prompted by disruption of tissue integrity in sarcopenia.

During development different types of MPCs can be recognized depending on morphological and biochemical characteristics. However, the MPCs all express embryonic MHC (Edom-Vovard *et al.*, 1999). Embryonic MHC is the first MHC isoform to be produced in the developing hind limb muscles, followed by more mature isoforms in a specific pattern depending on the location and function of the skeletal muscle studied (Ontell *et al.*, 1993). Embryonic myosin is re-expressed in adult skeletal muscle under a number of experimental conditions. However, these conditions share the property of inducing regeneration of muscle tissue. This is also the case for re-expression of embryonic myosin after denervation, which has been studied extensively by the group of Carlson (Borisov *et al.*, 2001). In the aged rat muscle we observed a dramatic increase in the number of MHCe-positive fibers, in particular in cases with advanced sarcopenia. This new piece of evidence shows that the regenerative effort in senescent muscle produces fibers that progress far into their program of maturation (Ontell *et al.*, 1993). Based on the relation of MHCe to behavioral symptoms, we conclude that regenerative activity as such does not seem to resolve the underlying problems in sarcopenia. Rather, increased regenerative efforts seem to be an indicator of poor outcome. Thus, the finding of increased MHC in sarcopenia suggests that investigative efforts should be directed towards factors that cause tissue damage or impaired tissue maintenance as well as poor efficiency and outcome of regeneration.

The early expression of immature MHC isoforms, including embryonic MHC, seems to be maintained in the absence of innervation, while the final maturation of MHC expression is innervation dependent (Crow & Stockdale, 1986; Yoshimura *et al.*, 1998; Adams *et al.*, 1999; Sacks *et al.*, 2003). Combined, these observations may indicate that in cases with an unsuccessful pattern of aging, advanced sarcopenia is at least in part due to a disturbed innervation of regenerating fibers (Jacob & Robbins, 1990; Clark & White, 1991; Kawabuchi *et al.*, 1998). A similar protracted maturation from regenerating to fully mature myofibers is seen in response to inflicted tissue damage in aged rodents (Brooks & Faulkner, 1994), a phenomenon that is also reflected in the prolonged IGF elevation seen after muscle injury in aged rodents (Marsh *et al.*, 1997). In addition, regenerating myofibers are initially in a more fragile state and have a reduced functional capacity (Renault *et al.*, 2000), which may contribute to the progression of sarcopenia. In experiments designed to elucidate whether a decreased capacity to re-innervate skeletal muscle in senescence has its origin in impairment of the target muscle or in the parent motoneurons, young hosts proved better than old at innervating an aged muscle (Carlson & Faulkner,

1989; Carlson *et al.*, 2001). In this context it is interesting to note that aged skeletal muscle expresses increased levels of several growth factor signaling components associated with re-innervation, such as IGF-I (this study), GDNF (Ming *et al.*, 1999a) and CNTF receptor  $\alpha$  (B. Ulfhake *et al.*, unpublished data) while growth factors such as neurotrophin 4, associated with muscle usage, are down-regulated (Ming *et al.*, 1999b; Jiang *et al.*, 2003). Moreover, aged motoneurons disclose a regenerative-like gene-expression profile (reviewed by Ulfhake *et al.*, 2000). The notion that sarcopenia has its origin in impaired innervation due to loss of, rather than decreased innervation by, motoneurons still awaits substantiation by unbiased counting of motoneuron numbers in well-fixed tissue (reviewed by Ulfhake *et al.*, 2000).

### Factors that may contribute to sarcopenia

Although not specifically addressed in this study, a number of factors may play important roles in muscle tissue deterioration during aging. As mentioned above, muscle fibers contain post-mitotic nuclei and are thus subject to wear and tear over extended periods of time. Environmental factors may drive the imbalance in muscle damage and repair during aging. In particular, metabolism and muscle usage may be important. Dietary (caloric) restriction (DR) has a beneficial effect, slowing the appearance of many of the features characterizing aged muscle, including alterations of energy and protein metabolism (Weindruch, 1995; Lee *et al.*, 1999). DR appears to reduce the baseline production of reactive oxygen species over time (Merry, 2002). This is also true for physical exercise (Ji, 2001), and several studies have shown positive effects of resistance training in the elderly (Rogers & Evans, 1993; Evans, 1996; Frischknecht, 1998; Roth *et al.*, 2000). Appropriate exercise probably provides a combination of stimuli to maintain tissue integrity during aging, including an influence on the local inflammatory response (Tidball, 2002) and paracrine/autocrine growth factor production (Goldspink & Yang, 2001). Successful regeneration is dependent on the local environment, including the extracellular matrix (ECM), to provide a more or less permissive milieu for growth and, thus, re-innervation (Tidball, 1995; Sanes, 2003). In this context, the capacity of the aged CNS to innervate regenerating fibers is of particular interest, because our data would be compatible with a disturbed maturation of regenerating muscle fibers, as discussed in the previous section.

Environmental influences as well as epigenetic modifications in all probability represent important modulators of the sarcopenia process. However, as with humans, aging rats show considerable variation in deficits among individuals, suggesting that genetic differences are important (Bergman & Ulfhake, 1998; Ulfhake *et al.*, 2002). In the outbred model used here, the animals age in a similar and well-controlled environment, which emphasizes the importance of the genetic background. Genomic differences between members of an age cohort probably play a key role in determining the pace and extent of sarcopenia under these conditions.

## Concluding remarks

A striking regenerative phenotype in sarcopenic skeletal muscle reflects a tissue in a state of continuous repair. Sarcopenia progresses in spite of a prominent proliferative activity in cases with an unsuccessful pattern of aging, a process that may be sustained by an impaired final maturation of regenerating myofibers into fully functional fibers. The combined effect of atrophy and loss of some myofibers combined with a state of regeneration in others, and, possibly, a retarded maturation of fibers implies a functionally impaired muscle with a decreased resistance to insult (Renault *et al.*, 2000). This vulnerability may promote further breakdown of muscle tissue in cases with pronounced sarcopenia.

## Experimental procedures

### Animals and tissue collection

Female Sprague–Dawley rats (strain Bkl; Harlan Sprague–Dawley, Houston, TX, USA), were delivered by a local breeder (B & K, Stockholm, Sweden) at 2 months of age and were thereafter kept under standardized barrier-housing conditions, under which the median lifespan is 30 months (Bergman, 1999). Thus, 30-month-old rats are herein defined as aged.

All rats were staged in relation to symptoms of impaired muscle function according to a previously described protocol (Johnson *et al.*, 1995). The rats were classified as having no or only minimal behavioral impairments (low symptom group, representing a 'successful' pattern of aging; 'AgL') or severely impaired (high symptom group, representing an unsuccessful pattern of aging; 'AgH'), including hind limb muscle atrophy (sarcopenia), adduction insufficiency, ataxia, disturbed gait cycle and signs of muscle paralysis (Johnson *et al.*, 1995). In addition, the animals were subjected to a series of behavioral tests for further characterization of the age-related impairments (Johnson *et al.*, 1995; Bergman & Ulfhake, 1998).

For tissue removal, chloral hydrate (300 mg kg<sup>-1</sup> i.p.) was used to induce deep anesthesia. Before tissue removal, body weights were recorded. Triceps surae muscles were quickly dissected out and gastrocnemius and soleus muscles were frozen separately in liquid nitrogen. Special care was taken to remove the soleus muscle from tendon to tendon. In total, ten young (2 months old), 30 adult (4 months old), 11 adult (12 months old) and 25 aged (30 months old) rats were used in this study. The 2- and 12-month-old rats were used only to provide reference data for the sarcopenia index (see below). For technical and practical reasons not all samples could be used for all analyses. The number of animals used for each analysis is listed under its subheading.

All experiments were approved by the Local Ethical Committee (Stockholms Norra Djurförsöksetiska Nämnd; project nos. N54/00 and N90/97) and conducted in accordance with Swedish law and regulations.

### Sarcopenia index

The relation between body weight and the mass of the postural soleus muscle was used to evaluate the adaptation of hind limb muscle to its weight-bearing demands at chosen points during the rodent lifespan. Whole soleus muscles were weighed from ten young (2-month-old), ten 4-month-old adult, 11 12-month-old adult and 20 aged (30-month-old) rats. For the statistical analysis, the aged rats were subdivided into AgL ( $n = 12$ ) and AgH ( $n = 8$ ) groups depending on their staging result. All soleus muscles, after being removed and frozen in liquid nitrogen, were weighed in one session in a cold room. An index, referred to in the text as the sarcopenia index, between soleus muscle weight (mg) and whole body weight (g) was created and is presented in Fig. 1.

### Behavioral testing

In total, 30 adult (4-month-old) and 25 aged (30-month-old) female Sprague–Dawley rats were tested. The aged rats were staged as previously described into AgL ( $n = 16$ ) and AgH ( $n = 9$ ) groups. All animals were subjected to the following tests.

#### *Open field activity*

Explorative behavior was examined with the open field test (Dorce & Palermo-Neto, 1994; Peng *et al.*, 1994; Drago *et al.*, 1996). In dim light, the animal was placed in the center of the arena (70 × 70 cm), which was divided into 25 equally large squares (14 × 14 cm), and allowed to explore freely for 180 s, during which the following behavioral characteristics were recorded: (a) number of squares entered with all four paws, (b) rearing frequency, (c) immobility frequency, and (d) instances of urination and defecation. The last measures (d) were recorded to provide a measure of anxiety level.

#### *Crossing a wire mesh screen*

A 70-cm-long wire mesh (2.5 cm) screen was used. In dim light, the animal was placed at one end of the screen and a 60-W light source was directed to this spot. The 'home cage' with litter mates was placed at the other end of the screen. Each animal was given 90 s to cross the screen. Records included distance, time and number of errors, i.e. instances of misplaced hind paws (slips).

#### *Beam balance*

A 2.5-cm-wide wooden beam was suspended 0.5 m above a soft surface. The rat was placed on the beam for a maximum of 60 s and the performance was ranked according to the following scale (Clifton *et al.*, 1991): (1) balances with steady posture and keeps its paws on top of the beam; (2) grasps sides of beam and/or has shaky movement; (3) one or more paws slip off beam; (4) attempts to balance on beam but falls; (5) drapes over beam and/or hangs on beam and falls off; (6) falls off beam with no attempt to balance or hang on. Each animal was subjected to three consecutive trials and the mean score of these trials was calculated.

### Walking track analysis

For this test, the animals' feet were immersed in non-toxic acrylic color (fore paws with red and hind paws with black color) and they then had to walk through an 8.5 × 42-cm transparent Plexiglas runway with the 'home cage' at the other end. High-quality paper was placed on the runway floor and taken out for analysis after the animal had crossed the path. The following records were made from the walking tracks: (a) stride length (distance between fore paw–fore paw and hind paw–hind paw), (b) gait width (distance between left and right hind paws) and (c) placement of hind paw relative to fore paw (distance between hind paw and fore paw in each step cycle).

### Righting response

The rat was held in the examiner's hand approximately 30 cm above a soft surface and the righting reflex was elicited by quickly turning the rat over on its back. The rat's attempt to right itself during the drop was studied and a score of 2 was given if the animal showed a normal righting response, i.e. counter to the roll direction; a score of 1 was given if the righting response was weak, delayed or in the direction of the roll; a score of 0 indicated no righting attempt (Gale *et al.*, 1985; von Euler *et al.*, 1996).

### RNA extraction and PCR

Using the Trizol®-protocol (GibcoBRL, Life Technologies, Täby, Sweden) total RNA was extracted from the gastrocnemius muscle of ten adult (4-month-old) and 15 aged (30-month-old) rats, of which eight belonged to the AgL and seven to the AgH groups. RNA purity and amount was measured spectrophotometrically (Pharmacia Ultraspec-plus, Uppsala, Sweden). Tissue analysis on a 10-ng sample of total RNA and of relative mRNA levels in gastrocnemius muscle was performed using reverse transcription (RT) and real-time polymerase chain reaction (real-time PCR). The reverse transcription was performed in a GeneAmp 2400 (Applied Biosystems, Stockholm, Sweden) using standard RT reagents (Applied Biosystems). The real-time PCR was carried out on 2 µL of the RT product (cDNA transcribed from 10 ng total RNA), with standard SYBR green mastermix (Applied Biosystems) and the appropriate primer pairs in an ABI-Prism

7000 instrument (Applied Biosystems). Details of the real-time PCR primers are given in Table 1. The IGF-I primer pair covers a region (in the pre-pro IGF-I region) common to all IGF-I splice variants and, thus, is a measure of total IGF-I mRNA. β-actin was used as an internal control. Real-time analysis of SYBR green fluorescence allows relative quantification of template (cDNA) amount through comparison of number of cycles needed to reach a defined signal level, typically the detection threshold. Thus, data for comparison of expression levels are given in numbers of cycles at detection threshold. These cycle numbers represent the exponential growth from cycle to cycle and should be treated as log-values. Normalization is consequently carried out through subtraction of the β-actin values.

Correct melting temperature and size of the amplified products were confirmed using melting curves and electrophoresis, respectively. The melting temperatures of a given product can be assessed in the ABI prism 7000 instrument through a gradual increase in temperature with concomitant signal detection. SYBR green has intense fluorescence only when DNA products are double stranded. When the melting temperature is reached the strands will dissociate and the signal intensity drops. Consequently, the drop in signal occurs at the melting point, allowing confirmation of the same melting curve for all compared products. Ten microliters of the PCR reaction product was electrophoresed alongside a DNA size standard on a 1.5% agarose gel containing ethidium bromide. The gels were visualized in a UV-transilluminator.

### Immunohistochemistry and counterstaining

The soleus muscles of nine adult (4-month-old) and 16 aged (30-month-old) rats, with the latter subdivided into AgL ( $n = 9$ ) and AgH ( $n = 7$ ) groups, were transversely sectioned in a cryostat and thawed onto gelatin/chrome-alun-coated slides. All sections except those used for MHCe quantification were then processed according to the indirect immunofluorescence technique. Briefly, the sections were rehydrated in PBS and then incubated for 18–72 h at 4 °C in a humid chamber with the primary antibodies diluted in PBS containing Triton-X100 (0.3%), sodium azide (0.01%) and Bacitracin (0.02%). The following primary antibodies, all from Novocastra Laboratories Ltd

**Table 1** Real-time PCR primer pairs

Target	Upper primer		Lower primer		Product (bp)	GenBank accession no.
	Position	Sequence	Position	Sequence		
Pre-pro IGF-I	80–97	GCGCACCTCCAATAAAGA	117–138	GAGTGCCAGGTAGAAGAGATGT	272	M15480
IGF-IR	483–506	CGCTGACCTCTGTACCTCTCCAC	895–913	TCTCGGCGTTGGGGATGTT	431	M27293
IGFbp5	1196–1217	CCCAACTGTGACCGCAAAGGAT	1328–1347	TCGAAGGCGTGGCACTGAAA	152	NM012817
Myf-5	75–97	GGATGAGTTTGGGGACCAAGTTT	429–451	GTCCCGGCAGGCTGTAATAGTTC	377	X56182
MyoD	3715–3735	GACGCCGCTACTACAGTGAG	4277–4298	GTAATCGGATTGGGCTTTGAG	269	M84176
Myogenin	694–712	ACCATGCCCCAACTGAGATT	862–880	TGGGCAGGGTGTAGTCTT	187	M24393
MRF4	629–649	GGGCCTGGTGATACTGCTAA	684–703	GAAAGCGCTGAAGACTGCT	75	M27151
β-actin	2232–2251	TCGTACCACTGGCATTGTGAT	2443–2464	CGAAGTCTAGGGCAACATAGCA	233	V01217

(Newcastle upon Tyne, UK), were used to identify muscle fiber isoforms based on myosin heavy chain (MHC) content: mouse anti-fast isoform, MHCf (diluted 1 : 50); mouse anti-slow isoform, MHCs (diluted 1 : 10) and mouse anti-developmental/embryonic isoform, MHCe (diluted 1 : 50). A rabbit polyclonal antibody raised against laminin (diluted 1 : 800, Sigma, St Louis, MO, USA) was used to identify the basement membrane. Tissue inflammatory cells were identified with monoclonal antibodies raised against ED1 and ED2 (both diluted 1 : 500 and from Serotec Ltd, Oxford, UK). ED1 recognizes the rat equivalent of human CD68 antigen expressed on cells of the myeloid lineage, including the majority of tissue macrophages. ED2 recognizes the rat equivalent of human CD163 antigen, which is expressed on a subset of macrophages.

Antibodies directed against IGF-I and IGF-R (Groppe, Australia), proline hydroxylase (fibroblast marker, Medicorp, Montréal, Canada) and MyoD (Novocastra) failed to produce reproducible immunohistochemical labeling.

After incubation with the primary antibodies, the sections were rinsed in PBS, transferred to a humid chamber and incubated at 37 °C for 30 min with FITC- or rhodamine-conjugated goat anti-rabbit or goat anti-mouse (1 : 80; Jackson Immuno Research Laboratories Inc., West Grove, PA, USA) antibodies. The sections were counterstained by immersion for 5 min in 0.001% propidium iodide (Sigma Aldrich) in distilled water, and subsequently rinsed in distilled water. The sections were mounted in glycerol/PBS (3 : 1) containing 1,4-diazabicyclo[2,2,2]octane in order to retard fading.

For quantification of MHCe-positive fibers it was preferable to use a non-fluorescent staining technique. The Vectastain elite® avidin–biotin complex (ABC, Vector Laboratories Inc., Burlingame, CA, USA) technique with diaminobenzidine (DAB, Sigma) detection was therefore used for this purpose. The protocol was run in parallel with the standard protocol up to the addition of the secondary antibody. A biotin-conjugated donkey anti-mouse secondary antibody was used [1.5 h incubation at room temperature (RT)]. During this time the ABC components (vial A and B of the kit) containing horseradish peroxidase (HRP) were mixed (both diluted 1 : 500) and left at RT until application (1.5 h incubation at RT) to the sections after secondary antibody incubation and rinsing. Detection was subsequently performed through pre-incubation of the rinsed sections with DAB solution (10-mg tablet per 25 mL of solution; Sigma) for 5 min followed by incubation using DAB solution with H<sub>2</sub>O<sub>2</sub> to catalyse the conversion by HRP of DAB to an insoluble detectable product. After rinsing, the sections were dehydrated in a series of alcohol dilutions and mounted with Entellan® (Merck, Darmstadt, Germany).

Negative control experiments where primary antibodies were omitted were routinely performed and made it possible to detect non-specific secondary antibody signals. The immunofluorescence tissue sections were examined with a Nikon Microphot-FX epifluorescence microscope (×10/0.45 and ×20/0.75 dry planapochromat objectives) equipped with the appropriate filters for FITC, rhodamine or propidium iodide fluorescence. Images were captured with a Nikon DXM1200 or with a Bio-Rad Radiance

Plus confocal microscope (×10/0.45 or ×20/0.75 dry planapochromat objectives or ×60/1.4 oil-immersion planapochromat objective). For MHCe quantitation, overview images of whole soleus muscle cross-sections were captured using a ×2/0.1 planapochromat objective. The overviews were used as templates and opened in Illustrator 10 (Adobe). Immunopositive fibers were then identified, confirmed microscopically and marked in the software to allow summation after all fibers were identified.

## Statistics

All statistics were performed using Statistica 6.1 (Statsoft, Tulsa, OK, USA). Comparisons of adult, aged low symptom and aged high symptom groups were carried out with parametric or non-parametric testing depending on the data type. Interval and ratio variables with an approximately normal distribution (sarcopenia index, real-time RT-PCR results and MHCe fiber counts) were tested using ANOVA (analysis of variance) and, when significant differences were found, Bonferroni's *post-hoc* test was used for pairwise comparisons. Log-transformation was performed when needed to meet the criteria of the ANOVA method. Ordinal data (behavior analysis data) were tested using Kruskal–Wallis non-parametric analysis of variance. When the initial test was significant, pairwise comparisons using Statistica's multiple comparisons were performed (comparison of mean ranks, Siegel & Castellan, 1988). Statistical significance levels were set to: \**P* < 0.05, \*\**P* < 0.01 and \*\*\**P* < 0.001. Boxplots used in Figs 1 and 2 were plotted using the following definitions: box limits represent upper and lower quartile values and are separated by the median (crossbar within box). The interquartile distance thus contains 50% of the data. Maximum and minimum values, which are not defined as outliers, are illustrated using error bars. Outliers (circles) are defined as values deviating from the quartile borders by more than 1.5× the interquartile distance.

## References

- Adams GR, Haddad F (1996) The relationships among IGF-1, DNA content, and protein accumulation during skeletal muscle hypertrophy. *J. Appl. Physiol.* **81**, 2509–2516.
- Adams GR, McCue SA, Zeng M, Baldwin KM (1999) Time course of myosin heavy chain transitions in neonatal rats: importance of innervation and thyroid state. *Am. J. Physiol.* **276**, R954–R961.
- Allen DL, Monke SR, Talmadge RJ, Roy RR, Edgerton VR (1995) Plasticity of myonuclear number in hypertrophied and atrophied mammalian skeletal muscle fibers. *J. Appl. Physiol.* **78**, 1969–1976.
- Allen DL, Yasui W, Tanaka T, Ohira Y, Nagaoka S, Sekiguchi C, Hinds WE, Roy RR, Edgerton VR (1996) Myonuclear number and myosin heavy chain expression in rat soleus single muscle fibers after spaceflight. *J. Appl. Physiol.* **81**, 145–151.
- Andersen JL, Terzis G, Kryger A (1999) Increase in the degree of co-expression of myosin heavy chain isoforms in skeletal muscle fibers of the very old. *Muscle Nerve* **22**, 449–454.
- Barton-Davis ER, Shoturma DI, Musaro A, Rosenthal N, Sweeney HL (1998) Viral mediated expression of insulin-like growth factor I blocks the aging-related loss of skeletal muscle function. *Proc. Natl Acad. Sci. USA* **95**, 15603–15607.

- Bergman E (1999) *Changes in Sensory Systems During Aging: an Experimental Study in the Rat*. Stockholm: Repro Print AB.
- Bergman E, Ulfhake B (1998) Loss of primary sensory neurons in the very old rat: neuron number estimates using the disector method and confocal optical sectioning. *J. Comp. Neurol.* **396**, 211–222.
- Borisov AB, Dedkov EI, Carlson BM (2001) Interrelations of myogenic response, progressive atrophy of muscle fibers, and cell death in denervated skeletal muscle. *Anat. Rec.* **264**, 203–218.
- Brooks SV, Faulkner JA (1994) Skeletal muscle weakness in old age: underlying mechanisms. *Med. Sci. Sports Exerc.* **26**, 432–439.
- Caccia MR, Harris JB, Johnson MA (1979) Morphology and physiology of skeletal muscle in aging rodents. *Muscle Nerve* **2**, 202–212.
- Carlson BM, Dedkov EI, Borisov AB, Faulkner JA (2001) Skeletal muscle regeneration in very old rats. *J. Gerontol. A Biol. Sci. Med. Sci.* **56**, B224–B233.
- Carlson BM, Faulkner JA (1989) Muscle transplantation between young and old rats: age of host determines recovery. *Am. J. Physiol.* **256**, C1262–C1266.
- Chambers RL, McDermott JC (1996) Molecular basis of skeletal muscle regeneration. *Can. J. Appl. Physiol.* **21**, 155–184.
- Chan K, Spencer EM (1997) General aspects of insulin-like growth factor binding proteins. *Endocrine* **7**, 95–97.
- Clark KI, White TP (1991) Neuromuscular adaptations to cross-reinnervation in 12- and 29-mo-old Fischer 344 rats. *Am. J. Physiol.* **260**, C96–C103.
- Clifton GL, Jiang JY, Lyeth BG, Jenkins LW, Hamm RJ, Hayes RL (1991) Marked protection by moderate hypothermia after experimental traumatic brain injury. *J. Cereb. Blood Flow Metab.* **11**, 114–121.
- Coschigano KT, Clemmons D, Bellush LL, Kopchick JJ (2000) Assessment of growth parameters and life span of GHR/BP gene-disrupted mice. *Endocrinology* **141**, 2608–2613.
- Crow MT, Stockdale FE (1986) Myosin expression and specialization among the earliest muscle fibers of the developing avian limb. *Dev. Biol.* **113**, 238–254.
- Dedkov EI, Kostrominova TY, Borisov AB, Carlson BM (2003) MyoD and myogenin protein expression in skeletal muscles of senile rats. *Cell Tissue Res.* **311**, 401–416.
- Dorce VA, Palermo-Neto J (1994) Behavioral and neurochemical changes induced by aging in dopaminergic systems of male and female rats. *Physiol. Behav.* **56**, 1015–1019.
- Drago F, Coppi G, Antonuzzo PA, Valerio C, Genazzani AA, Grassi M, Raffaele R, Scapagnini U (1996) Effects of RGH 2202 on cognitive and motor behavior of the rat. *Neurobiol. Aging* **17**, 67–71.
- Dutta C, Hadley EC (1995) The significance of sarcopenia in old age. *J. Gerontol. A Biol. Sci. Med. Sci.* **50**, Spec. No., 1–4.
- Edom-Vovard F, Mouly V, Barbet JP, Butler-Browne GS (1999) The four populations of myoblasts involved in human limb muscle formation are present from the onset of primary myotube formation. *J. Cell Sci.* **112**, 191–199.
- von Euler M, Akesson E, Samuelsson EB, Seiger A, Sundstrom E (1996) Motor performance score: a new algorithm for accurate behavioral testing of spinal cord injury in rats. *Exp. Neurol.* **137**, 242–254.
- Evans WJ (1995) What is sarcopenia? *J. Gerontol. A Biol. Sci. Med. Sci.* **50**, Spec. No., 5–8.
- Evans WJ (1996) Reversing sarcopenia: how weight training can build strength and vitality. *Geriatrics* **51**, 46–47, 51–43; quiz 54.
- Foulstone EJ, Meadows KA, Holly JM, Stewart CE (2001) Insulin-like growth factors (IGF-I and IGF-II) inhibit C2 skeletal myoblast differentiation and enhance TNF alpha-induced apoptosis. *J. Cell Physiol.* **189**, 207–215.
- Friedlander AL, Butterfield GE, Moynihan S, Grillo J, Pollack M, Holloway L, Friedman L, Yesavage J, Matthias D, Lee S, Marcus R, Hoffman AR (2001) One year of insulin-like growth factor I treatment does not affect bone density, body composition, or psychological measures in postmenopausal women. *J. Clin. Endocrinol. Metab.* **86**, 1496–1503.
- Frischknecht R (1998) Effect of training on muscle strength and motor function in the elderly. *Reprod. Nutr. Dev.* **38**, 167–174.
- Gale K, Kerasidis H, Wrathall JR (1985) Spinal cord contusion in the rat: behavioral analysis of functional neurologic impairment. *Exp. Neurol.* **88**, 123–134.
- Goldspink G, Yang SY (2001) Effects of activity on growth factor expression. *Int. J. Sport Nutr. Exerc. Metab.* **11** (Suppl.), S21–S27.
- Greenlund LJ, Nair KS (2003) Sarcopenia – consequences, mechanisms, and potential therapies. *Mech. Ageing Dev.* **124**, 287–299.
- Gutman B, Hanzlikova V (1972) *Age Changes in the Neuromuscular System*. Bristol: Scientifica Ltd.
- Hamilton MT, Marsh DR, Criswell DS, Lou W, Booth FW (1995) No effect of aging on skeletal muscle insulin-like growth factor mRNAs. *Am. J. Physiol.* **269**, R1183–R1188.
- Hasty P, Bradley A, Morris JH, Edmondson DG, Venuti JM, Olson EN, Klein WH (1993) Muscle deficiency and neonatal death in mice with a targeted mutation in the myogenin gene. *Nature* **364**, 501–506.
- Hawke TJ, Garry DJ (2001) Myogenic satellite cells: physiology to molecular biology. *J. Appl. Physiol.* **91**, 534–551.
- Hikida RS, Van Nostran S, Murray JD, Staron RS, Gordon SE, Kraemer WJ (1997) Myonuclear loss in atrophied soleus muscle fibers. *Anat. Rec.* **247**, 350–354.
- Holzenberger M (2004) The GH/IGF-I axis and longevity. *Eur. J. Endocrinol.* **151** (Suppl. 1), S23–S27.
- Jacob JM, Robbins N (1990) Age differences in morphology of reinnervation of partially denervated mouse muscle. *J. Neurosci.* **10**, 1530–1540.
- Jette AM, Jette DU (1997) Functional and behavioral consequences of sarcopenia. *Muscle Nerve Suppl.* **5**, S39–S41.
- Ji LL (2001) Exercise at old age: does it increase or alleviate oxidative stress? *Ann. NY Acad. Sci.* **928**, 236–247.
- Jiang X, Edstrom E, Altun M, Ulfhake B (2003) Differential regulation of Shc adaptor proteins in skeletal muscle, spinal cord and forebrain of aged rats with sensorimotor impairment. *Aging Cell* **2**, 47–57.
- Johnson H, Mossberg K, Arvidsson U, Piehl F, Hokfelt T, Ulfhake B (1995) Increase in alpha-CGRP and GAP-43 in aged motoneurons: a study of peptides, growth factors, and ChAT mRNA in the lumbar spinal cord of senescent rats with symptoms of hindlimb incapacities. *J. Comp. Neurol.* **359**, 69–89.
- Kablar B, Krastel K, Ying C, Asakura A, Tapscott SJ, Rudnicki MA (1997) MyoD and Myf-5 differentially regulate the development of limb versus trunk skeletal muscle. *Development* **124**, 4729–4738.
- Kawabuchi M, Chongjian Z, Islam AT, Hirata K, Nada O (1998) The effect of aging on the morphological nerve changes during muscle reinnervation after nerve crush. *Restor. Neurol. Neurosci.* **13**, 117–127.
- Klitgaard H, Bergman O, Betto R, Salvati G, Schiaffino S, Clausen T, Saltin B (1990) Co-existence of myosin heavy chain I and IIa isoforms in human skeletal muscle fibres with endurance training. *Pflugers Arch.* **416**, 470–472.
- Larsson L (1978) Morphological and functional characteristics of the ageing skeletal muscle in man: a cross-sectional study. *Acta Physiol. Scand. Suppl.* **457**, 1–36.
- Launay T, Armand AS, Charbonnier F, Mira JC, Donsez E, Gallien CL, Chanoine C (2001) Expression and neural control of myogenic regulatory factor genes during regeneration of mouse soleus. *J. Histochem. Cytochem.* **49**, 887–899.
- Lee CK, Klopp RG, Weindruch R, Prolla TA (1999) Gene expression profile of aging and its retardation by caloric restriction. *Science* **285**, 1390–1393.
- Lexell J (1995) Human aging, muscle mass, and fiber type composition. *J. Gerontol. A Biol. Sci. Med. Sci.* **50**, Spec. No. 11–16.

- Lieberman SA, Hoffman AR (1997) The somatopause: should growth hormone deficiency in older people be treated? *Clin. Geriatr. Med.* **13**, 671–684.
- Ludolph DC, Konieczny SF (1995) Transcription factor families: muscling in on the myogenic program. *FASEB J.* **9**, 1595–1604.
- Marcell TJ (2003) Sarcopenia: causes, consequences, and preventions. *J. Gerontol. A Biol. Sci. Med. Sci.* **58**, M911–M916.
- Marsh DR, Criswell DS, Hamilton MT, Booth FW (1997) Association of insulin-like growth factor mRNA expressions with muscle regeneration in young, adult, and old rats. *Am. J. Physiol.* **273**, R353–R358.
- McQueeney K, Dealy CN (2001) Roles of insulin-like growth factor-I (IGF-I) and IGF-I binding protein-2 (IGFBP2) and -5 (IGFBP5) in developing chick limbs. *Growth Horm. IGF Res.* **11**, 346–363.
- Merry BJ (2002) Molecular mechanisms linking calorie restriction and longevity. *Int. J. Biochem. Cell Biol.* **34**, 1340–1354.
- Ming Y, Bergman E, Edstrom E, Ulfhake B (1999a) Evidence for increased GDNF signaling in aged sensory and motor neurons. *Neuroreport* **10**, 1529–1535.
- Ming Y, Bergman E, Edstrom E, Ulfhake B (1999b) Reciprocal changes in the expression of neurotrophin mRNAs in target tissues and peripheral nerves of aged rats. *Neurosci. Lett.* **273**, 187–190.
- Musaro A, Cusella De Angelis MG, Germani A, Ciccarelli C, Molinaro M, Zani BM (1995) Enhanced expression of myogenic regulatory genes in aging skeletal muscle. *Exp. Cell Res.* **221**, 241–248.
- Musaro A, McCullagh K, Paul A, Houghton L, Dobrowolny G, Molinaro M, Barton ER, Sweeney HL, Rosenthal N (2001) Localized IGF-1 transgene expression sustains hypertrophy and regeneration in senescent skeletal muscle. *Nat. Genet.* **27**, 195–200.
- Ontell M, Ontell MP, Sopper MM, Mallonga R, Lyons G, Buckingham M (1993) Contractile protein gene expression in primary myotubes of embryonic mouse hindlimb muscles. *Development* **117**, 1435–1444.
- Peng YI, Lin SH, Chen TJ, Tai MY, Tsai YF (1994) Effects of age on open-field behavior of male rats. *Chinese J. Physiol.* **37**, 233–236.
- Porter MM, Vandervoort AA, Lexell J (1995) Aging of human muscle: structure, function and adaptability. *Scand. J. Med. Sci. Sports* **5**, 129–142.
- Rawls A, Wilson-Rawls J, Olson EN (2000) Genetic regulation of somite formation. *Curr. Top. Dev. Biol.* **47**, 131–154.
- Renault V, Piron-Hamelin G, Forestier C, DiDonna S, Decary S, Hentati F, Saillant G, Butler-Browne GS, Mouly V (2000) Skeletal muscle regeneration and the mitotic clock. *Exp. Gerontol.* **35**, 711–719.
- Robertson TA, Papadimitriou JM, Grounds MD (1993) Fusion of myogenic cells to the newly sealed region of damaged myofibers in skeletal muscle regeneration. *Neuropathol. Appl. Neurobiol.* **19**, 350–358.
- Rogers MA, Evans WJ (1993) Changes in skeletal muscle with aging: effects of exercise training. *Exerc. Sport Sci. Rev.* **21**, 65–102.
- Rosenberg IH (1997) Sarcopenia: origins and clinical relevance. *J. Nutr.* **127**, 990S–991S.
- Roth SM, Ferrell RF, Hurley BF (2000) Strength training for the prevention and treatment of sarcopenia. *J. Nutr. Health Aging* **4**, 143–155.
- Rotwein P, James PL, Kou K (1995) Rapid activation of insulin-like growth factor binding protein-5 gene transcription during myoblast differentiation. *Mol. Endocrinol.* **9**, 913–923.
- Roubenoff R, Castaneda C (2001) Sarcopenia – understanding the dynamics of aging muscle. *J. Am. Med. Assoc.* **286**, 1230–1231.
- Rudnicki MA, Schlegelsberg PN, Stead RH, Braun T, Arnold HH, Jaenisch R (1993) MyoD or Myf-5 is required for the formation of skeletal muscle. *Cell* **75**, 1351–1359.
- Sacks LD, Cann GM, Nikovits W Jr, Conlon S, Espinoza NR, Stockdale FE (2003) Regulation of myosin expression during myotome formation. *Development* **130**, 3391–3402.
- Sanes JR (2003) The basement membrane/basal lamina of skeletal muscle. *J. Biol. Chem.* **278**, 12601–12604.
- Severgnini S, Lowenthal DT, Millard WJ, Simmen FA, Pollock BH, Borst SE (1999) Altered IGF-I and IGFBPs in senescent male and female rats. *J. Gerontol. A, Biol. Sci. Med. Sci.* **54**, B111–B115.
- Siegel S, Castellan NJ (1988) *Nonparametric Statistics for the Behavioral Sciences*. New York: McGraw-Hill.
- Sjogren K, Liu JL, Blad K, Skrtic S, Vidal O, Wallenius V, LeRoith D, Tornell J, Isaksson OG, Jansson JO, Ohlsson C (1999) Liver-derived insulin-like growth factor I (IGF-I) is the principal source of IGF-I in blood but is not required for postnatal body growth in mice. *Proc. Natl Acad. Sci. USA* **96**, 7088–7092.
- Smith TH, Block NE, Rhodes SJ, Konieczny SF, Miller JB (1993) A unique pattern of expression of the four muscle regulatory factor proteins distinguishes somitic from embryonic, fetal and newborn mouse myogenic cells. *Development* **117**, 1125–1133.
- Tajbakhsh S, Rocancourt D, Buckingham M (1996) Muscle progenitor cells failing to respond to positional cues adopt non-myogenic fates in myf-5 null mice. *Nature* **384**, 266–270.
- Tidball JG (1995) Inflammatory cell response to acute muscle injury. *Med. Sci. Sports Exerc.* **27**, 1022–1032.
- Tidball JG (2002) Interactions between muscle and the immune system during modified musculoskeletal loading. *Clin. Orthop.* **403**, S100–S109.
- Tomonaga M (1977) Histochemical and ultrastructural changes in senile human skeletal muscle. *J. Am. Geriatr. Soc.* **25**, 125–131.
- Tureckova J, Wilson EM, Cappalonga JL, Rotwein P (2001) Insulin-like growth factor-mediated muscle differentiation. collaboration between phosphatidylinositol 3-kinase-akt-signaling pathways and myogenin. *J. Biol. Chem.* **276**, 39264–39270.
- Ulfhake B, Bergman E, Edstrom E, Fundin BT, Johnson H, Kullberg S, Ming Y (2000) Regulation of neurotrophin signaling in aging sensory and motoneurons: dissipation of target support? *Mol. Neurobiol.* **21**, 109–135.
- Ulfhake B, Bergman E, Fundin BT (2002) Impairment of peripheral sensory innervation in senescence. *Auton. Neurosci.* **96**, 43–49.
- Vandromme M, Rochat A, Meier R, Carnac G, Besser D, Hemmings BA, Fernandez A, Lamb NJ (2001) Protein kinase B beta/Akt2 plays a specific role in muscle differentiation. *J. Biol. Chem.* **276**, 8173–8179.
- Weindruch R (1995) Interventions based on the possibility that oxidative stress contributes to sarcopenia. *J. Gerontol. A Biol. Sci. Med. Sci.* **50**, Spec. No., 157–161.
- Williamson DL, Godard MP, Porter DA, Costill DL, Trappe SW (2000) Progressive resistance training reduces myosin heavy chain coexpression in single muscle fibers from older men. *J. Appl. Physiol.* **88**, 627–633.
- Yoshimura K, Kuzon WM, Harii K (1998) Myosin heavy chain expression in skeletal muscle autografts under neural or aneural conditions. *J. Surg. Res.* **75**, 135–147.
- Yun K, Wold B (1996) Skeletal muscle determination and differentiation: story of a core regulatory network and its context. *Curr. Opin. Cell Biol.* **8**, 877–889.